

# The First Stars in The Universe

S. Naoz, S. Noter and R. Barkana<sup>1</sup> \*

<sup>1</sup>*School of Physics and Astronomy, The Raymond and Beverly Sackler Faculty of Exact Sciences, Tel Aviv University, Tel Aviv 69978, ISRAEL*

4 October 2018

## ABSTRACT

Large telescopes have allowed astronomers to observe galaxies that formed as early as 850 million years after the Big Bang. We predict when the first star that astronomers can observe (i.e., in our past light cone) formed in the universe, accounting for the first time for the size of the universe and for three essential ingredients: the light travel time from distant galaxies, Poisson and density fluctuations on all scales, and the effect of very early cosmic history on galaxy formation. We find that the first observable star is most likely to have formed 30 million years after the Big Bang (at redshift 65). Also, the first galaxy as massive as our own Milky Way likely formed when the universe was only 400 Myr old (at redshift 11). We also show that significant modifications are required in current methods of numerically simulating the formation of galaxies at redshift 20 and above.

**Key words:** galaxies:high-redshift – cosmology:theory – galaxies:formation

## 1 INTRODUCTION

The formation of the first stars, in a universe that had not yet suffered chemical and magnetic stellar feedback, is a well-defined problem for theorists (Barkana, & Loeb 2001). The advent of large telescopes has accelerated the observational quest for the first objects as astronomers have detected the light emitted by increasingly distant galaxies (Fan, et al. 2003). A theoretical understanding of the first stars is of great importance as observations approach the pristine regime of the early universe.

Stars are understood to form at high redshift out of gas that cooled and subsequently condensed to high densities in the cores of dark matter halos. Since metals are absent in the pre-stellar universe, the earliest available coolant is molecular hydrogen ( $H_2$ ), and thus the minimum halo mass that can form a star is set by requiring the infalling gas to reach a temperature  $\gtrsim 1000$  K required for exciting the rotational and vibrational states of  $H_2$  (Tegmark et al. 1997). This has been confirmed with high-resolution numerical simulations containing gravity, hydrodynamics, and chemical processes in the primordial gas (Abel, Bryan & Norman 2002; Bromm, Coppe & Larson 2002). These simulations showed that the first star formed within a halo containing  $\sim 10^5 M_\odot$  in total mass; however, as we show, they could not estimate *when* the first star formed.

## 2 LIMITATIONS OF SIMULATIONS

In the real universe, the cosmological redshift  $z$  of each source implies a corresponding cosmic age at which the source is seen. Thus, the observable universe can be divided into thin spherical shells around us, each containing a portion of the universe that is observed at a given redshift  $z$  and is seen at the corresponding age. Galaxy formation in different shells is correlated due to density fluctuations on various scales. A simulation that wishes to determine when various objects are observed to form must encompass a sufficient portion of our past light cone.

Even with adaptive grid codes, full simulations are limited by current technology to tiny regions and only form a first star below redshift 20 (Abel, Bryan & Norman 2002) or 33 for the most recent simulations (O’Shea & Norman 2006). Even when great sacrifices are made in the realism, so that hydrodynamics and chemical evolution are neglected and the collapse of a star is only partially resolved, simulations still cannot capture the proper cosmological context. A direct simulation of the universe out to the spherical shell at redshift 70 would require a simulated box of length 25,000 Mpc on a side [measured in comoving distance, which equals physical distance times a factor of  $(1+z)$ ]. The need to resolve each  $10^5 M_\odot$  halo into 500 particles (required to determine the halo’s evolution even crudely (Springel & Hernquist 2003)) determines the mass of each simulated particle, while the mean cosmic density of  $4 \times 10^{10} M_\odot/\text{Mpc}^3$  yields the total mass of the simulated box, and implies a required total of  $3 \times 10^{21}$  particles. The maximum number achieved thus far is only  $\sim 10^{10}$  (Springel et al. 2005). Early times have been probed by res-

\* E-mail: smadar@wise.tau.ac.il (SN); shaynote@post.tau.ac.il (SN); barkana@wise.tau.ac.il (RB)

imulating regions from a large initial simulation (Reed et al. 2005), forming star-forming halos at  $z = 47$  (the earliest to date), but with cosmological parameters for which the first galaxy actually formed at  $z \sim 82$  according to our model below. Thus, the actual starting redshift of the era of galaxy formation can currently only be predicted analytically. For similar parameters, Miralda-Escudé (2003) made a rough analytical estimate (using the Press & Schechter (1974) halo mass function) and found that the first star formed at  $z \sim 48$ . A rough estimate by Wise & Abel (2005) found  $z \sim 71$  using the improved Sheth & Tormen (1999) mass function (see also § 3).

Simulations of the first stars also face a difficulty in the way their initial conditions are determined. Recent observations of the cosmic microwave background (CMB) (Spergel et al. 2006) have confirmed the notion that the present large-scale structure in the universe as well as the galaxies within it originated from small-amplitude density fluctuations at early cosmic times. Simulations thus assume Gaussian random initial fluctuations as might be generated by a period of cosmic inflation in the early universe. The evolution of these fluctuations can be calculated exactly as long as they are small, with the linearized Einstein-Boltzmann equations. The need to begin when fluctuations are still linear forces numerical simulations of the first star-forming halos to start at a high redshift, the highest to-date being 600 (Reed et al. 2005). Current simulations neglect the contribution of the radiation to the expansion of the universe and assume the Newtonian limit of general relativity which is valid in simulation boxes that are small with respect to the horizon. However, for a halo that forms around redshift 65, we find below that the corresponding region already must have had a moderately non-linear overdensity of  $\delta \sim 20\%$  at  $z = 600$  ( $\delta$  is the density perturbation divided by the cosmic mean density). Indeed, we find that for initial conditions that ensure 1% accuracy in  $\delta$ , simulations must start deep in the radiation dominated era, at  $z > 10^6$ . Furthermore, we show that a small error in  $\delta$  leads to a much larger error in the abundance of halos at each redshift. The non-linearity of the initial conditions represents a previously-unrecognized fundamental limitation of current methods of simulating the formation of the first star-forming halos.

### 3 SPHERICAL COLLAPSE

While numerical simulations cannot determine the formation time of the first observable star, galaxy and halo formation can also be understood and described with a standard analytical model that has been quantitatively checked with simulations where the latter are reliable. The standard analytical model for the abundance of halos (Press & Schechter 1974; Bond, Cole, Efstathiou & Kaiser 1991) considers the linear density fluctuations at some early, initial time, and attempts to predict the number of halos that will form at some later time corresponding to a redshift  $z$ . First, the fluctuations are evolved to the redshift  $z$  using the equations of linear fluctuations, i.e., they are artificially linearly extrapolated even if they may become non-linear in some regions. The average density is then computed in spheres of various sizes. Whenever the overdensity in a sphere containing mass  $M$  rises above a critical threshold  $\delta_c(M, z)$ ,

the corresponding region is assumed to have collapsed by redshift  $z$ , forming a halo of at least mass  $M$ . Thus, the model separates the linear growth of fluctuations, which we calculate with standard codes (Seljak & Zaldarriaga 1996; Naoz & Barkana 2005; Yamamoto, Sugiyama & Sato 1998), from the non-linear collapse of objects, which determines the effective linear threshold  $\delta_c(M, z)$ .

Within this model, the non-linear collapse of a halo is analyzed by considering a uniform, spherically symmetric fluctuation whose collapse can be calculated by numerically solving ordinary differential equations;  $\delta_c(M, z)$  is then determined as the value of the linearly-extrapolated  $\delta$  of the spherical region at the moment when the actual, non-linear  $\delta$  diverges (i.e., the region collapses to a point). The classical calculation of spherical collapse in an Einstein de-Sitter (EdS) universe (i.e., a flat matter-dominated universe) yields  $\delta_c = 1.686$ , a value that is independent of the halo mass and the collapse redshift (Gunn & Gott 1972). Given the power spectrum of the initial fluctuations, together with their linear growth, we can determine the chance that regions containing various initial masses  $M$  will reach the threshold  $\delta_c$  at some final redshift  $z$ , and this forms the basis for estimating the abundance of halos of mass  $M$  that form at a specific  $z$  (Press & Schechter 1974; Bond, Cole, Efstathiou & Kaiser 1991). We use the recently-modified form of this model [Sheth & Tormen (1999), with the updated parameters suggested by Sheth & Tormen (2002)], which fits halo abundances in numerical simulations very accurately in regimes that include  $M = 10^{11} - 10^{15} M_\odot$  halos at  $z = 0 - 10$  (Jenkins et al. 2001; Springel et al. 2005) and  $M = 10^6 M_\odot$  halos at  $z = 15 - 30$  (Barkana & Loeb 2004; Yoshida, et al. 2003). We note that other suggested mass functions (e.g., Reed et al. 2006) are in agreement with the Sheth & Tormen (1999) mass function if the updated parameters are used. Based on the plausible physical arguments behind this model together with its quantitative success out to redshift 30, we extrapolate it to predict halo abundances at still-higher redshifts.

Our results assume cosmological parameters matching the latest CMB and weak lensing observations (Spergel et al. 2006). For the contributions to the energy density, we assume ratios relative to the critical density of  $\Omega_m = 0.299$ ,  $\Omega_\Lambda = 0.701$ , and  $\Omega_b = 0.0478$ , for matter, cosmological constant, and baryons, respectively. We also assume a Hubble constant  $H_0 = 100h \text{ km s}^{-1} \text{ Mpc}^{-1}$  with  $h = 0.687$ , and a primordial power-law power spectrum with spectral index  $n = 0.953$  and  $\sigma_8 = 0.826$ , where  $\sigma_8$  is the root-mean-square amplitude of mass fluctuations in spheres of radius  $8 h^{-1} \text{ Mpc}$ .

Within this analytical model, we can account for early cosmic history when predicting the abundance of high-redshift stars and galaxies. We first calculate the correct value of  $\delta_c(M, z)$  with a spherical collapse calculation that includes the full formation history of each halo (Figure 1), starting out with a small perturbation and following its gravitational evolution until it collapses. We begin our calculation at a very high redshift when  $\delta \ll 1$ , which implies that the overdense region containing the mass  $M$  is larger than the horizon. In this regime we use the cosmological Friedmann equations of general relativity, applied to the overdense region that we are following. We begin in the

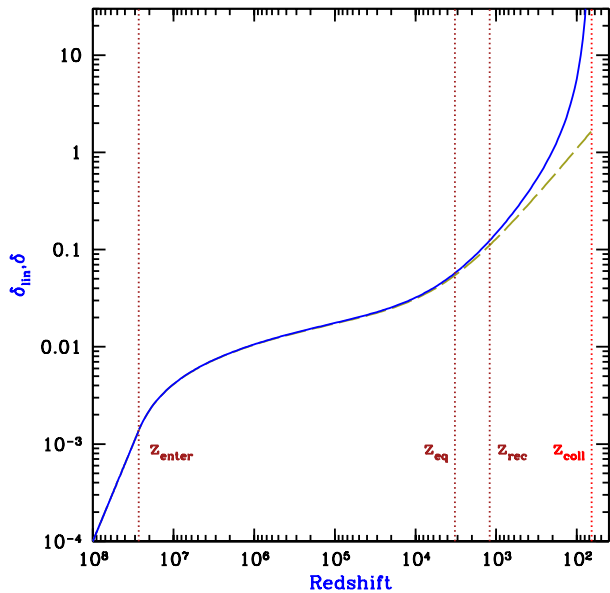


**Figure 1.** Evolution of the fractional overdensity  $\delta$  for a spherical region containing  $10^5 M_\odot$  that collapses at  $z = 66$ . We show the fully non-linear  $\delta$  (solid curve) and the linearly-extrapolated  $\delta$  (dashed curve). We indicate the redshifts of halo collapse ( $z_{\text{coll}}$ ), cosmic recombination ( $z_{\text{rec}}$ ), matter-radiation equality ( $z_{\text{eq}}$ ), and entry into the horizon ( $z_{\text{enter}}$ ).

radiation-dominated era, and include throughout the contribution of the radiation to the cosmic expansion. Once the fluctuation enters the horizon, the overdense dark matter continues to collapse due to gravity, but the radiation pressure suppresses the sub-horizon perturbation in the photon density, and the coupling of the baryons to the photons (via Compton scattering) keeps the baryon perturbation small as well. Thus, in this regime we neglect the perturbation in the radiation and baryons and continue to evolve the spherical collapse of the dark matter perturbation. The formation of hydrogen at cosmic recombination ( $z \sim 1200$ ) decouples the cosmic gas from its mechanical drag on the CMB, and the baryons (which constitute a significant 17% of all the matter) subsequently begin to fall into the pre-existing gravitational potential wells of the dark matter. In this regime we evolve the coupled collapse of the dark matter and the baryons, both evolving under their mutual gravity but with different initial conditions. We find that a halo destined to contain the first observable star in the universe reaches a  $\delta \sim 1\%$  at  $z \sim 10^6$  and grows to  $\delta \sim 6\%$  at matter-radiation equality and  $\delta \sim 13\%$  at cosmic recombination. Since the fluctuation enters the horizon very early in the radiation-dominated era, the final value of  $\delta_c(M, z)$  for a given  $M$  and  $z$  is insensitive to the precise starting redshift (as long as it is much higher than equality) or the precise treatment of the fluctuation's horizon crossing.

We find that  $\delta_c$  is essentially independent of  $M$ , and for our assumed parameters it is lower than the EdS value by  $\sim 1\% \times (1+z)/20$  in the range  $z = 9-80$ . Adding the contribution of the radiation to the expansion of the universe, as well as adding the baryon-photon coupling to the collapse, both reduce the extrapolated linear perturbation

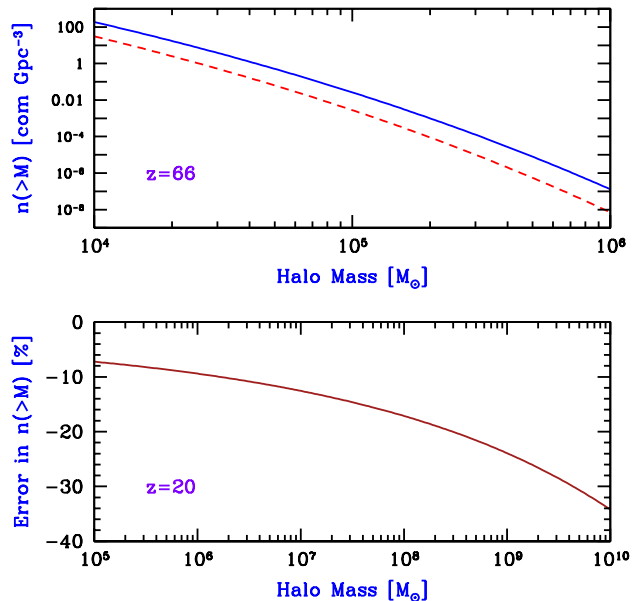


**Figure 2.** Cumulative halo mass function  $n(> M)$ . At  $z = 66$  (top panel) we compare our full result for  $n(> M)$  (solid curve) to that resulting from adopting the EdS value of  $\delta_c = 1.686$  (dashed curve). At  $z = 20$  (bottom panel), we show the relative error in  $n(> M)$  that results from using  $\delta_c = 1.686$  instead of our full result.

at collapse  $\delta_c$  compared with the EdS value. These added physical effects reduce the collapse efficiency since only the dark matter component takes part in the collapse throughout. The radiation is kept smooth by its own pressure and it never participates in the collapse, while the baryons only gradually recover from their coupling to the photons and begin to catch up to the dark matter; during this recovery stage, as long as the baryon perturbations remain much smaller than those of the dark matter, the baryons essentially do not participate in the collapse. Now, any reduction in the matter fraction that collapses (compared to 100% in the usually-assumed case of pure cold dark matter) depresses the linear evolution of the density perturbation more strongly, while the non-linear perturbation is larger and is thus less affected by the components that do not help in the collapse. Therefore the linear perturbation reaches a lower value of  $\delta_c$  when the non-linear perturbation collapses. Note that while the change in  $\delta_c$  may seem small, when dealing with rare halos, even a change of a few percent in  $\delta_c$  can change the halo abundance at a given redshift by an order of magnitude (Figure 2). Even at redshift 20, the 1% change in  $\delta_c$  compared to its previously-assumed value changes the cumulative halo mass function  $n(> M)$  by  $\gtrsim 10\%$ .

#### 4 STATISTICAL CONSIDERATIONS

As noted earlier, the minimum halo mass that can form a star at high redshift is determined by  $H_2$  cooling (Tegmark et al. 1997). Numerical simulations (Abel, Bryan & Norman 2002; Bromm, Coppe & Larson 2002; Fuller & Couchman, 2000; Yoshida, et al. 2003; Reed et al. 2005) imply a minimum circular velocity  $V_c \sim$

4.5 km/s, where  $V_c = \sqrt{GM/R}$  in terms of the halo virial radius  $R$ . This yields a corresponding minimum mass at each redshift  $z'$ ,  $M_{\min}(z')$ . The simulations show that in a halo above the minimum mass, the gas cools in the dense center and forms at least one star very quickly; this is understood theoretically since both the cooling time and the dynamical time are a small fraction of the cosmic age at that time.

Given the comoving number density of such star-forming halos at each redshift,  $n(M_{\min}(z'), z')$ , the mean expected number of star-forming halos observed at redshift  $z$  or higher is

$$\langle N \rangle(z) = \int_z^{z_{\max}} n(M_{\min}(z'), z') \frac{dV}{dz'} dz', \quad (1)$$

where  $dV$  is the comoving volume of the spherical shell in the redshift range  $z'$  to  $z' + dz'$ . Our results are independent of the adopted maximum redshift as long as  $z_{\max} > 80$ . Although the mean expected number  $\langle N \rangle(z)$  is determined theoretically by the cosmological parameters, in practice our observable universe presents us with a single instance and the actual observed redshift is subject to Poisson and density fluctuations.

The effect of Poisson fluctuations is easily calculated. The chance of observing at least one star-forming halo above redshift  $z$  with Poisson fluctuations included is  $1 - \exp[-\langle N \rangle(z)]$ , which yields a spread in the redshift of the first such halo of  $\Delta z \approx 3$  at  $1 - \sigma$ . In addition, the effect of density fluctuations on all scales is included statistically in our analytical model for the mean halo abundance at each redshift, but the correlations in the halo abundance between nearby points are not properly included. In other words, our calculation assumes that the relevant redshift shell gives us a fair sample of the density fluctuations on all scales. We first note that theoretically we expect that if we included the fully correlated density field, the effect on the predicted redshift of the first star-formation halo would be much smaller than the spread we find due to Poisson fluctuations. Since the universe is homogeneous on large scales, large-scale modes can shift the halo abundance  $\langle N \rangle(z)$  only by a small  $\Delta z$ ; indeed, only 10 Mpc scales and smaller can produce a  $\Delta z > 1$  (Barkana & Loeb 2004). Such small-scale modes are indeed very well sampled within the spherical redshift shells that have a very large radius of  $\sim 12,500$  Mpc. We have also verified this with a direct quantitative test. We have used the power spectrum to produce instances of the full, correlated density field in three-dimensional boxes. We have then modified the abundance  $n(M_{\min}(z), z)$ , increasing it in high-density regions and decreasing it in low-density regions according to a model that fits the results of numerical simulations (Barkana & Loeb 2004). In a  $1 \text{ Gpc}^3$  box resolved into  $256^3$  cells, we found that including a correlated density field shifts the typical redshift of the first star-forming halo in the box by a  $\Delta z < 1$ , which is already a smaller effect than the Poisson redshift spread. The spherical shells in the real universe have a larger volume by a factor of  $\sim 2000$ , so the density fluctuations are far better sampled than in our  $1 \text{ Gpc}^3$  box, and the effect of the correlations on the redshift of the first star-forming halo in the universe is negligible.

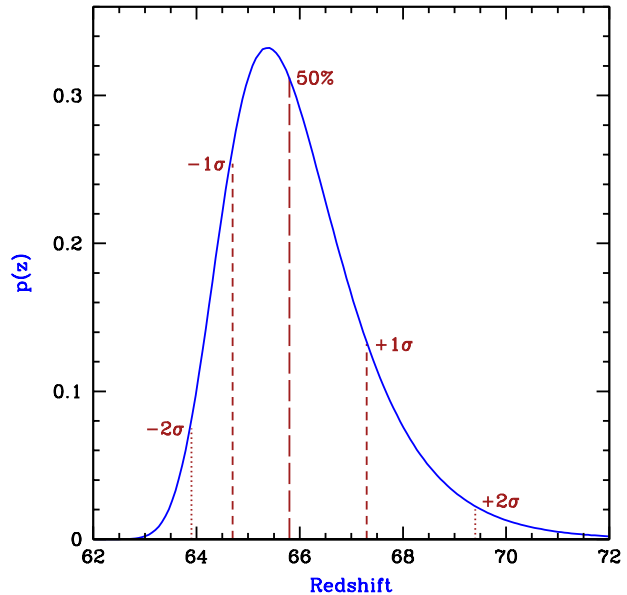


**Figure 3.** The probability of finding the first star as a function of redshift. Vertical lines show the median redshift as well as the central  $1 - \sigma$  (68%) range and  $2 - \sigma$  (95%) range.

## 5 PREDICTIONS

The most likely redshift for the first observable star is 65.4 (Figure 3), while the median redshift at which there is a 50% chance of seeing the first star is 65.8, which corresponds to a cosmic age of  $t = 31$  Myr, less than a quarter of one percent of the current age of 13.7 Gyr. The  $1 - \sigma$  (68%) range is  $z = 64.7 - 67.3$  (or  $t = 30 - 32$  Myr) and the  $2 - \sigma$  (95%) range is  $z = 63.9 - 69.4$ . Note that even an error in the minimum  $V_c$  as large as a factor of 1.5 would cause only a 9% change in the expected formation redshift. Note also that in terms of the total cosmic mass fraction contained in such halos, the first star-forming halo corresponds to an  $8.3 - \sigma$  density fluctuation on the mass scale of  $10^5 M_\odot$ . Future simulations will allow us to check the validity of extrapolating the Sheth & Tormen (1999) halo mass function to such rare fluctuations.

We can consider a similar question for other populations of halos (Figure 4). For example, the radiation from the first stars is expected to eventually dissociate all the  $H_2$  in the intergalactic medium, leading to the domination of a second generation of larger galactic halos where the gas cools via radiative transitions in atomic hydrogen and helium (Haiman, Rees, & Loeb 1997). Atomic cooling occurs in halos with  $V_c > 16.5$  km/s, in which the infalling gas is heated above 10,000 K and is ionized. We find that the first galaxy to form via atomic cooling formed at  $z = 46.6_{-0.9}^{+1.2}$ , which corresponds to  $t = 52_{-2}^{+1}$  Myr, where we have indicated the median values and  $1 - \sigma$  ranges. We also predict that the first halo as large as that of our own Milky Way galaxy (Battaglia et al. 2005) formed at  $z = 11.1_{-0.2}^{+0.5}$ , or  $t = 408_{-20}^{+15}$  Myr. Also, the first halo with the mass of the Coma galaxy cluster (Lokas & Mamon 2003) formed at  $z = 1.24_{-0.10}^{+0.14}$ , or  $t = 5.0 \pm 0.4$  Gyr.

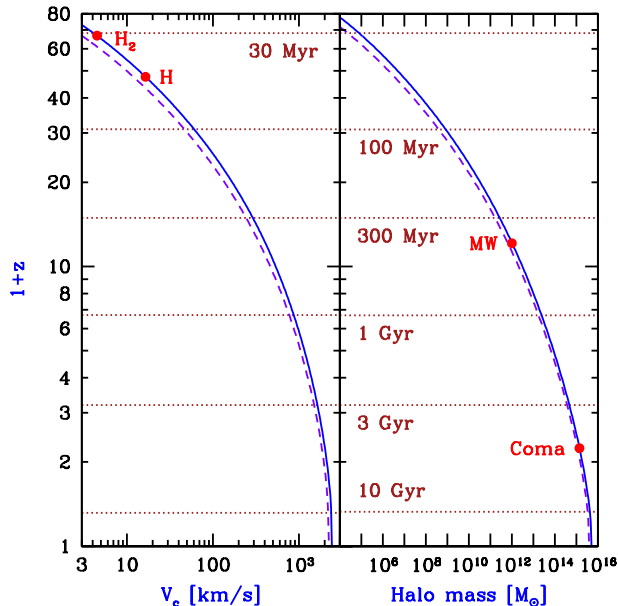


**Figure 4.** The median redshift for the first appearance of various populations of halos. We consider halos above a minimum circular velocity (left panel) or minimum mass (right panel). We indicate in particular the first star-forming halo in which  $H_2$  allows the gas to cool, the first galaxy that forms via atomic cooling ( $H$ ), as well as the first galaxy as massive as our own Milky Way and the first cluster as massive as Coma. The horizontal lines indicate the elapsed time since the Big Bang. We compare the results with the cosmological parameters from Spergel et al. (2006) [solid curve] to those with the parameters from Viel et al. (2006) [dashed curve]; the difference represents roughly the systematic  $1\sigma$  error due to current uncertainties in the values of the cosmological parameters.

## 6 DISCUSSION

There remains a  $\sim 10\%$  systematic uncertainty in the above  $1+z$  values due to current uncertainties in the cosmological parameters. Varying the cosmological parameters has a negligible effect on the critical overdensity ( $\delta_c$ ) but significantly changes the power spectrum and also the spatial scale corresponding to a given halo mass or circular velocity. We illustrate the uncertainties in Figure 4 using the alternate cosmological parameters from Viel et al. (2006):  $\Omega_m = 0.253$ ,  $\Omega_\Lambda = 0.747$ ,  $\Omega_b = 0.0425$ ,  $h = 0.723$ ,  $n = 0.957$  and  $\sigma_8 = 0.785$ . These parameters also represent typical  $1-\sigma$  errors, in terms of the parameters uncertainties given by Spergel et al. (2006). We obtained for these alternate parameters that the first star formed at  $z = 60.0$ , which represents a 9% reduction in  $1+z$  compared to our standard parameters; also the value of  $1+z$  is lowered by 9% for the first atomic-cooling halo, 7% for the first Milky Way-mass halo, and 8% for the first Coma-mass cluster.

On the other hand, astrophysical uncertainties about metallicity and feedback can only affect the precise properties of a halo of a given mass, but not whether or not it forms. Also, in a halo with a short cooling time, processes within the halo should not induce a significant uncertainty in the formation time of the first stars within it, since a halo virializes at a density of  $\sim 180$  times the cosmic mean density, and so the gravitational dynamical time within it is

always smaller than the age of the universe at the time by at least an order of magnitude. Since the baryonic component collapses by another factor of  $\sim 20$  until the collapse is halted by angular momentum (assuming a typical halo spin parameter of  $\sim 5\%$ ; see, e.g., Mo, Mao, & White (1998)), the dynamical time within a disk or a star-forming region is likely to be shorter still by another two orders of magnitude.

In summary, by accounting for the size of the observable universe as well as the early cosmic history of individual halos (Figure 1), our results extend the era of star formation much earlier than current simulations suggest. An analytical model of galaxy formation that has been normalized to simulation results allows us to predict the earliest time that various halo populations can be observed (Figure 4). Since the statistical uncertainty in this time is dominated by Poisson fluctuations, we can analytically predict its full probability distribution (Figure 3). Our results also show that in order to numerically simulate galaxy formation accurately at  $z \geq 20$ , current simulation methods must be revised to include the effect on a forming halo of the early cosmic history of radiation and baryons. Simulations that neglect this, even if they overcome the statistical challenges by covering the volume of the entire observable universe, will underestimate the number of halos at  $z = 20$  (Figure 2) by 9% for all halos above the  $H_2$  cooling threshold ( $6 \times 10^5 M_\odot$  at  $z = 20$ ), and by 15% for all halos above the atomic cooling threshold ( $3 \times 10^7 M_\odot$  at  $z = 20$ ).

## ACKNOWLEDGMENTS

The authors acknowledge support by Israel Science Foundation grant 629/05 and U.S. - Israel Binational Science Foundation grant 2004386.

## REFERENCES

- Abel, T. L., Bryan, G. L., & Norman, M. L. 2002, *Science* 295, 93
- Barkana, R., & Loeb, A. 2001, *Phys. Rep.* 349, 125
- Barkana, R., & Loeb, A. 2004, *ApJ.*, 609, 474
- Battaglia, G., et al. 2005, *MNRAS*, 364, 433
- Bond, J. R., Cole, S., Efstathiou, G., & Kaiser, N. 1991, *ApJ* 379, 440
- Bromm, V., Coppie, P. S., & Larson, R. B. 2002, *ApJ*, 564, 23
- Fan, X., et al. 2003, *AJ*, 125, 1649
- Fuller, T. M., & Couchman, H. M. P. 2000, *ApJ*, 544, 6
- Gunn, J. E., & Gott, J. R. 1972, *ApJ*, 176, 1
- Haiman, Z., Rees, M. J., & Loeb, A. 1997 *ApJ*, 484, 985
- Jenkins, A., et al. 2001, *MNRAS*, 321, 372
- Lokas, E. L., & Mamon, G. A. 2003, *MNRAS*, 343, 401
- Miralda-Escudé J., 2003, *Sci*, 300, 1904
- Mo H. J., Mao S., White S. D. M., 1998, *MNRAS*, 295, 319
- Naoz, S., & Barkana, R. 2005, *MNRAS*, 362, 1047
- O’Shea, B. W., & Norman, L. 2006, preprint astro-ph/0607013
- Press, W. H., & Schechter, P., A. 1974, *ApJ*, 187, 425
- Reed, D. S., et al. 2005, *MNRAS*, 363, 393
- Reed, D. S., et al. 2006, astro-ph 0607150
- Seljak, U., & Zaldarriaga, M. 1996, *ApJ*, 469, 437

- Sheth, R. K., & Tormen, G. 1999, MNRAS, 308, 119  
Sheth R. K., & Tormen G., 2002, MNRAS, 329, 61  
Spergel, D. N., et al. 2006, preprint astro-ph/0603449  
Springel, V., & Hernquist, L. 2003, MNRAS, 339, 312  
Springel, V. et al. 2005, Nature, 435, 629  
Tegmark, M., et al. 1997, ApJ, 474, 1  
Viel M., Haehnelt M. G., & Lewis, A. 2006, MNRAS, 370,  
L51  
Wise J. H., Abel T., 2005, ApJ, 629, 615  
Yamamoto, K., Sugiyama, N., & Sato, H. 1998, ApJ, 501,  
442  
Yoshida, N., Sokasian, A., Hernquist, L., & Springel, V.  
2003, ApJ, 598, 73

This paper has been typeset from a  $\text{\TeX}$ / $\text{\LaTeX}$  file prepared by the author.